

# Flutter in Webs

Peter M. Moretti

<http://www.mae.okstate.edu/Faculty/moretti/moretti.html>

T.U. Darmstadt, den 28.X.2002

## Abstract

Unter der Rubrik “Fluid/Structure Interaction” gibt es zahlreiche Probleme von Schwingungen in Luftfahrt, Hydraulik, und Wärmetauschern die von der Strömung erregt werden. Ein klassisches Beispiel, mit Anwendung auf Papier- und Druckmaschinen, ist das Flattern von Fahnen:

- 1.) Wann wird die Fahne instabil?
- 2.) Warum wird die Last an der Befestigung dann viel größer?
- 3.) Was begrenzt die Amplitude der Schwingungen?

Eine lineare “gyroskopische” Gleichung wird entwickelt um die erste Frage zu beantworten. Die Dynamik der entstehenden Schwingungen wird benutzt, um die entstehende Spannung zu erklären. Vorläufige Forschungsergebnisse zur dritten Frage werden angedeutet.

Die Anwendung zur Lösung von Problemen in Papiermaschinen wird gezeigt.

## 1 Overview

Flow-induced vibrations can be categorized in various ways, for example into internal or external flows, and into longitudinal or transverse flows. Three of the more interesting types of fluid/structure interaction are

1. Wing or control-surface flutter in airplanes. These generally involve two different motion, flapping and twisting, which occur ninety degrees out-of-phase. The two oscillatory motions are dynamically coupled because the structural center, the center of gravity, and the center of lift are at different locations within the wing. The motion extracts energy from the flow and puts it into vibration of the structure.
2. Cross-flow on bluff bodies: for example, individual or well-spaced wires, such as the high-voltage transmission wires studied by Prof. Hagedorn; or cylindrical arrays, such as the tube bundles in shell-and-tube heat exchangers.<sup>1</sup> Depending on the values of the similitude parameters, a whole range of different physical processes can be involved, including

---

<sup>1</sup>Peter M. Moretti, “Flow-Induced Vibrations in Arrays of Cylinders,” *Annual Review of Fluid Mechanics*, Volume 25, pages 99–114, Jan. 1993, ISSN: 0066-4189.

- (a) random excitation by free-field turbulence (Owens);
- (b) vortex-shedding (Y.N. Chen);
- (c) galloping and jet-switching (B.W. Roberts);
- (d) fluid-elastic whirling (H.J. Connors);
- (e) single-cylinder flutter (Weaver & Abd-Rabo).

The fluid mechanics of the last of these, which must involve a time delay, has not been explained satisfactorily.

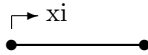
3. Axial flow on slender bodies, or along panels, sheets, or webs. Unlike the superficially similar phenomenon of water waves, the structural behavior of fluttering flags is not well understood, and will be discussed below.

## 2 Review of Fundamentals

### 2.1 The Wave Equation

The homogeneous form of the **governing equation** for a string, when normalized (but not yet made dimensionless to eliminate  $c$ ) has the basic form

$$\left[ \frac{\partial^2 w}{\partial t^2} \right]_{\xi=\text{const}} - c^2 \left[ \frac{\partial^2 w}{\partial \xi^2} \right]_{t=\text{const}} = 0 \quad (1)$$



where  $w$  is the lateral deflection of a string, and  $c^2 = (T/\rho A) = |\sigma/\rho|$ . The independent variable  $\xi$  measures location relative to a point on the string; the string must be either stationary, or else moving at a constant velocity and direction, so that the attached coordinate system is inertial.

This governing equation is satisfied by **traveling-wave** solutions, for example

$$z = C_1 \sin(\kappa\xi - \omega t) + C_2 \sin(\kappa\xi + \omega t)$$

where angular frequency  $\omega = 2\pi/\tau$  and wave-number  $\kappa = 2\pi/\lambda$  are related by  $\omega/\kappa = c$

$$z = C_1 \sin \kappa(\xi - ct) + C_2 \sin \kappa(\xi + ct)$$

Fixed end conditions generate negative reflections, so that the original state returns after  $\tau_1 = (2L/c)$ , when waves have reflected twice and traveled a total of two lengths.

Numerical **simulation** can be obtained from the finite-difference equation

$$\left[ \frac{w_{n,m+1} - 2w_{n,m} + w_{n,m-1}}{(\Delta t)^2} \right] - c^2 \left[ \frac{w_{n+1,m} - 2w_{n,m} + w_{n-1,m}}{(\Delta \xi)^2} \right] = 0$$

Assuming that we have two sets of older values of  $z$ , we solve for a new set of values

$$w_{n,m+1} \cong \left(\frac{c\Delta t}{\Delta\xi}\right)^2 w_{n+1,m} + 2\left(1 - \left(\frac{c\Delta t}{\Delta\xi}\right)^2\right) w_{n,m} + \left(\frac{c\Delta t}{\Delta\xi}\right)^2 w_{n-1,m} - w_{n,m-1}$$

but we must choose the relative step-sizes  $\Delta\xi/\Delta t = c$ ; larger  $\Delta t$  lead to numerical instability, and larger  $\Delta\xi$  lead to numerical diffusion (smearing of waveforms, or apparent-damping of modes).

For fixed end conditions, separation-of-variables gives standing-wave solutions in the form of **classical modes** such as

$$w = C \cos(\omega t) \times \sin(\kappa\xi)$$

where  $\kappa_n = n\pi/L$ , and therefore  $\omega_n = c \cdot \kappa_n = cn\pi/L$ .

Standing-wave solutions can always be expressed by **superposition** of traveling waves

$$\cos(\omega t) \times \sin(\kappa x) = \frac{1}{2} \sin(\kappa x - \omega t) + \frac{1}{2} \sin(\kappa x + \omega t)$$

but it is not possible to describe a single traveling wave as a classical mode  $\sin(\kappa\xi)$  or  $\text{Im}(e^{i\kappa\xi})$ ; instead we need a “neo-classical” complex-number mode

$$\begin{aligned} \sin(\kappa\xi \mp \omega t) &= \sin(\kappa\xi) \cos(\omega t) \mp \cos(\kappa\xi) \sin(\omega t) \\ &= \text{Im}(e^{i\kappa\xi}) \text{Re}(e^{i\omega t}) \mp \text{Re}(e^{i\kappa\xi}) \text{Im}(e^{i\omega t}) \\ &\Rightarrow \sin(\kappa\xi) \cos(\omega t) \pm i \cos(\kappa\xi) \sin(\omega t) \\ &= \cos(\omega t) [\sin(\kappa\xi) \pm i \cos(\kappa\xi)] \\ &= \sin(\omega t) [e^{\pm i\kappa\xi}] \end{aligned}$$

## 2.2 Varying Tension

If the tension  $T$  is not constant (due to gravity or drag forces), an additional tension-gradient term was pointed out by Drs. Chakraborty and DasGupta

$$\rho A \frac{\partial^2 w}{\partial t^2} - T \frac{\partial^2 w}{\partial \xi^2} - \frac{dT}{d\xi} \frac{\partial w}{\partial \xi} = 0$$

which still permits separation of variables, but requires solving for  $\omega^2$  after applying the end-conditions to the modal equation

$$T_{(\xi)} \frac{d^2 W}{d\xi^2} + \left(\frac{dT}{d\xi}\right) \frac{dW}{d\xi} + \rho A \omega^2 W = 0$$

## 2.3 Bending Stiffness

The equation can be expanded to include slender tensioned beams (and compressed columns) by adding the bending-stiffness term  $+(EI/\rho A) [\partial^4 w/\partial \xi^4]$ ,

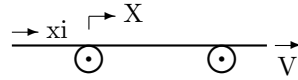
which makes the equation fourth-order. Traveling waves are now dispersive, because the speed of sinusoidal waves is not fixed, but depends on wave-length. Standing-wave solutions require hyperbolic in addition to trigonometric terms, except for a special case: simple pinned end conditions lead to simple sinusoidal modes, with natural frequencies

$$f_n = \frac{1}{2\pi} \sqrt{\left(\frac{n\pi}{L}\right)^2 \left(\frac{T}{\rho A}\right) + \left(\frac{n\pi}{L}\right)^4 \left(\frac{EI}{\rho A}\right)}$$

Evidently, the frequency goes to zero at the buckling load  $T = -(\pi/L)^2 EI$

### 3 Threadlines

If the string translates at a constant velocity  $V$  relative to the supports



the wave equation still applies, but it is convenient to transform to a coordinate  $x$  defined by

$$\begin{aligned} x - Vt &= \xi \\ x &\triangleq \xi + Vt \end{aligned}$$

in order to make the end-conditions stationary.<sup>2</sup> Transforming the simple wave equation, we obtain a **governing equation** with gyroscope-like terms which Prof. Markert's students will recognize as similar to Coriolis and centrifugal forces

$$\left[\frac{\partial^2 w}{\partial t^2}\right]_{x=\text{const}} + 2V \left[\frac{\partial^2 w}{\partial t \partial x}\right] + (V^2 - c^2) \left[\frac{\partial^2 w}{\partial x^2}\right] = 0 \quad (2)$$

where  $|V^2 - c^2|$  reflects an "apparent" tension/mass term. Reversing the coordinate directions changes only the sign of the mixed-derivative term. Stability requires that  $V^2 \leq c^2$ .

Relative to the new coordinate system  $x$ , the **traveling waves** are

$$\begin{aligned} w &= C_1 \sin \kappa_o ((x - Vt) - ct) + C_2 \sin \kappa_o ((x - Vt) + ct) \\ &= C_1 \sin \kappa_o (x - (c + V)t) + C_2 \sin \kappa_o (x + (c - V)t) \end{aligned}$$

progressing at the speed  $(c + V)$  in the direction of string travel, and at  $(c - V)$  in the opposite direction.

INSERT Fig.2 from Y.B.Chang, Fox, Lilley, & Moretti 1991

<sup>2</sup>Peter M. Moretti, *Modern Vibrations Primer*, CRC Press, Boca Raton, ©2000 (ISBN 0-8493-2038-0), page 302.

The original state returns when a wave and its reflections have travel one length  $L$  in each direction,

$$\tau_1 = \frac{L}{(c+V)} + \frac{L}{(c-V)} = \frac{2cL}{c^2 - V^2} = \left(\frac{2L}{c}\right) \left(\frac{c^2}{c^2 - V^2}\right)$$

Since no choice of  $\Delta x/\Delta t$  can be equal to both  $(c+V)$  and  $(c-V)$ , the simple central-difference scheme is always either unstable or else suffers from numerical diffusion: accurate numerical **simulation** is more difficult than in the string-bound coordinate  $\xi$ .

Simple separation of variables into functions of  $t$  and  $x$  is not possible because of the Coriolis-like term; **solutions with a modal envelope** have forms such as

$$w = C \cos\left(\left(\frac{c^2 - V^2}{c^2}\right)\omega_o t + \frac{V}{c}\kappa_o x\right) \times \sin(\kappa_o x)$$

which collapses to our standing-wave solution  $w = C \cos(\omega_o t) \times \sin(\kappa_o x)$  when  $V = 0$ , but describes a *traveling wave moving opposite to the traveling string, within a sinusoidal envelope*.

INSERT Fig.1a from Y.B.Chang, Fox, Lilley, & Moretti 1991

The fundamental frequency is

$$\frac{1}{\tau_1} = f_1 = \frac{1}{2\pi} \sqrt{\left(\frac{\pi}{L}\right)^2 \left(\frac{T}{\rho A}\right) \left(1 - \frac{V^2}{(T/\rho A)}\right)}$$

and the fundamental phase velocity is  $\left(\frac{c^2 - V^2}{c^2}\right)\omega_o \div \frac{V}{c}\kappa_o = \left(\frac{c^2 - V^2}{V}\right)$ . During one fundamental period  $\tau_1 = 2Lc/(c^2 - V^2)$ , the wave travels a distance  $2Lc/V$ .

Expressed in the string-bound coordinate  $\xi$ , the same solution would have been

$$w = \frac{C}{2} \sin\left(\left(\frac{c-V}{c}\right)\kappa_o(\xi - ct)\right) + \frac{C}{2} \sin\left(\left(\frac{c+V}{c}\right)\kappa_o(\xi + ct)\right)$$

which has the expected form  $\mathfrak{F}_1(\xi - ct) + \mathfrak{F}_2(\xi + ct)$ : the solution can always be expressed by **superposition** of traveling waves beating against each other. In the end-condition-bound coordinate  $x$ , this is

$$w = \frac{C}{2} \sin\left(\left(\frac{c-V}{c}\right)\kappa_o(x - (c+V)t)\right) + \frac{C}{2} \sin\left(\left(\frac{c+V}{c}\right)\kappa_o(x + (c-V)t)\right)$$

We can confirm that the frequency of each of the waves passing a fixed point  $x$  is

$$f_1 = \frac{1}{2\pi} \left(\frac{c^2 - V^2}{c^2}\right)\omega_o$$

Similar behavior can be found in flexible **hose-pipes** containing flowing fluids: the governing equation has the same general form

$$A \left[ \frac{\partial^2 w}{\partial t^2} \right] \pm 2B \left[ \frac{\partial^2 w}{\partial t \partial x} \right] \mp C \left[ \frac{\partial^2 w}{\partial x^2} \right] = 0$$

where  $A$  depends on the masses of the hose-pipe and the fluid;  $B$  on the mass and velocity of the fluid; and  $C$  on the mass and velocity of the fluid and on the tension  $T$ . Through normalization of the space- and/or the time-coordinate this can be reduced to an equation with a single dimensionless parameter

$$\ddot{w} + 2\beta \dot{w}' \mp w'' = 0$$

where the coefficient  $\beta = B/\sqrt{A \cdot C}$  can be made positive by choice of coordinate direction  $x$ . The sign of the last coefficient is determined by the magnitude of the tension (relative to dynamic effects) and must be negative for stability (i.e., the tension must be adequate).

## 4 Flow along a web

### 4.1 Slender strip

For longitudinal flow along a long, narrow web, drying air displaced by out-of-plane oscillations moves around the sides of the strip, and the apparent mass  $m_{air}$  (per-unit-length) added by the surrounding air is obtained from Lamb's hydrodynamic inertia coefficient for an infinite strip

$$m_{air} = \frac{\pi}{4} (\text{width})^2 \rho_{air}$$

The governing equations is<sup>3</sup>

$$(m_{web} + m_{air}) \left[ \frac{\partial^2 w}{\partial t^2} \right] + 2(m_{web} V_{web} + m_{air} V_{air}) \left[ \frac{\partial^2 w}{\partial t \partial x} \right] + (m_{web} V_{web}^2 + m_{air} V_{air}^2 - T) \left[ \frac{\partial^2 w}{\partial x^2} \right] = 0$$

and  $m_{air}$  is much larger than  $m_{web}$  in many practical situations.

The stability of this linear equation can be examined by writing exponential solutions and looking for positive-real exponents. Wind-tunnel tests were done for various values of  $T$  and  $V_{air}$ , with  $V_{web} = 0$

INSERT Fig.4 from Y.B.Chang, Fox, Lilley, & Moretti 1991

and both static divergence in the form of bulging

INSERT Fig.5 & Fig.6 from Y.B.Chang, Fox, Lilley, & Moretti 1991

and flutter oscillations were observed.

INSERT Fig.7 from Y.B.Chang, Fox, Lilley, & Moretti 1991

<sup>3</sup>view details in "Aerodynamics of moving belts, tapes, and webs" available as PDF-file on [www.mae.okstate.edu/Faculty/moretti/moretti.html](http://www.mae.okstate.edu/Faculty/moretti/moretti.html)

## 4.2 Short wave-lengths

For flow along a web or across the web, where the wave-length of the flutter oscillations is short compared to the other dimension of the web,<sup>4</sup> the hydrodynamic inertia is a function of the wavelength

$$m_{air} = \frac{\lambda}{\pi} \rho_{air}$$

Inserting this in the governing equation makes it pseudo-linear, but still useful for observing trends. An alternative is the classic aero-elasticity approach of iterating between (a.) solving for the response of the structure under the influence of the pressure-field created by the flow; and (b.) solving for the flow conforming to the surface of the structure. Since our structure is simply a tensioned string and/or beam, and the pressure results mainly from the far-field potential flow, the computation is fairly straight-forward.

## 4.3 Three-dimensional waves

While the slender-body and the short-wave-length limiting cases are convenient because they lead to cylindrical deflection-shapes, practical situations lead to three-dimensional modes.<sup>5</sup>

INSERT Fig.4 from Y.B.Chang & Moretti 2000

Combining a tensioned-membrane calculation with a potential-flow calculation is required to solve this problem. Cross-flow towards a slack edge turns out to be similar to flag flutter: there is very little tension (and very little stiffness), and the situations is generally unstable. There are two engineering options:

- either stabilize by introducing tension in some way, such as tension along the edge;
- or else predict and manage the amplitudes of the oscillation.

The latter motivates us to look at what controls post-critical-stability flutter oscillations in flags. What limits the amplitudes? Tension due to viscous drag, plate stiffness, etc. are all very small—are there structural non-linearities that come into play?

---

<sup>4</sup>see, for example, Y.B. Chang & P.M. Moretti, “An Experimental Study of Edge Flutter in Webs,” *Web Handling - 1992*, AMD-Vol. 149, pp. 67–78, American Society of Mechanical Engineers, N.Y. 1992, ASBN 0-7918-1104-2.

<sup>5</sup>Y.B. Chang & P.M. Moretti, “Flow-induced vibrations of free edges of thin films,” *Flow-Induced Vibration*, Proc. of the 7th Intl. Conf. on Flow-Induced Vibration (FIV2000), editors S. Ziada & T. Staubli, Luzern, 19–22 Juni 2000, pp.801–810; publisher Balkema, Rotterdam, ISBN 90-5809-129-5.

## 5 Flag Flutter

### 5.1 Background

When a flag flutters in a breeze, the trailing (leech) edge travels a curved path and develops centrifugal forces which stretch the flag. The resulting tension is felt at the attachment point (flag pole) like increased drag, over and above the drag due to boundary-layer friction. It accounts for the additional drag of a fluttering flag<sup>6</sup> relative to a similar-sized stiff panel.

Where the flag curves, the induced tension flattens the flag, opposing pressure differences between the opposite sides of the flag. These pressure differences are complementary to the potential-flow field around the flag. Thus the flow field around the flag generates forces normal to the flag, producing accelerations; the resulting velocities generate centrifugal forces which induce tension in the flag; and this tension opposes and ultimately limits the amplitudes of the flag motion.

This reciprocal process dynamically transform lift forces into drag. It can be studied or measured either from the structural and from the fluid side:

- from the structural side, we can analyze the dynamics of the flag (as we will do below), or measure the drag forces at the flagpole; and
- from the fluid side, we can analyze the flow field, or measure the velocity profile in the wake.

The drag force must, of course, balance the momentum defect in the wake.

### 5.2 Flutter-induced Tension

#### 5.2.1 Wave Form

Once flutter begins, additional tension is induced by the dynamic deflection  $w$  in the  $z$ -direction (normal to the initial plane of the flag). As an approximation, we use a simple description of the deflection  $w$  which captures the essential features of the observed motion: a *traveling wave* within an envelope<sup>7</sup> growing from a value of zero at the leading edge (where  $x = 0$ ) to the amplitude  $A$  at the trailing edge (where  $x = L$ ), for example in the simple form also used by Uno,<sup>8</sup> for the traveling wave

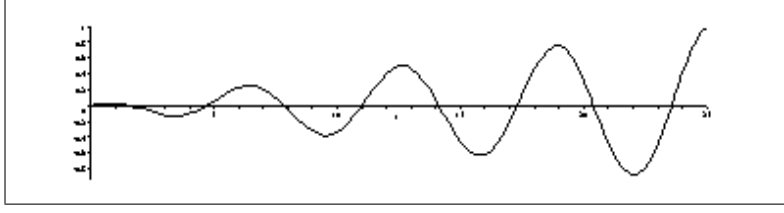
$$w = \frac{Ax}{L} \cos(\omega t - \kappa x)$$

---

<sup>6</sup>R.A. Fairthorne (1930), "Drag of Flags," *Aeronautical Research Committee (ARC) Reports and Memoranda No. 1345* (Ae.477), Her Majesty's Printing Office (HMSO), London, May 1930; pp. 887-891.

<sup>7</sup>D. Thoma (T.H. München), "Warum flattert die Fahne," Translation "Why does the flag flutter," Cornell Aeronautical Laboratory 1949.

<sup>8</sup>Minoru Uno, "Fluttering of Flexible Bodies," *Journal of the Textile Machinery Society of Japan*, Vol. 19, No. 4/5 (1973), pp. 103-109; also *JTMSJ, Transactions*, Vol. 26, No. 8 (1973), T73-79.



where  $A$  is the maximum amplitude;  $x$  is the distance along the flag measured from the support;  $L$  is the maximum value of  $x$ ; and the frequency of the waves is  $f = \omega/2\pi$ . In this first approximation,  $\kappa$  is taken to be a constant; therefore the *wave-length is assumed constant* at  $\lambda = 2\pi/\kappa$ ; and the phase velocity is also constant at  $c = f\lambda = \omega/\kappa$ . A more compact way of writing this is to define dimensionless time and lengths

$$t^* \triangleq \omega t$$

$$x^* \triangleq \kappa x$$

$$L^* \triangleq \kappa L$$

$$w^* \triangleq \kappa w$$

and the ratio

$$A_r \triangleq \frac{A}{L} = \frac{A^*}{L^*}$$

so that our chosen first-approximation mode is condensed into the dimensionless form

$$w^* = A_r x^* \cos(t^* - x^*)$$

### 5.2.2 Longitudinal Motion

The path length  $s$  of the wave to any location  $x$  is  $ds^* = \sqrt{(dx^*)^2 + (dw^*)^2}$ ; inserting our wave-form we obtain

$$s = \frac{1}{\kappa} \int_0^{x^*} \sqrt{1 + \{A_r [\cos(t^* - \xi) + x^* \sin(t^* - \xi)]\}^2} d\xi$$

and the  $u$ -deflection in the (negative)  $x$ -direction (parallel to the free-stream velocity) is  $u^* = (x^* - s^*)$ . Therefore the path of an element of the flag is described by the  $w$ -deflection normal to the reference plane, plus the  $u$ -deflection in the reference plane of the flag.

For moderate deflections and slopes, we can approximate the path-length expression with the first two terms of the binomial expansion

$$\begin{aligned} \frac{ds}{dx} &= \sqrt{1 + \left(\frac{dw}{dx}\right)^2} \cong 1 + \frac{1}{2} (dw/dx)^2, \text{ if } (dw/dx)^2 \ll 1 \\ &\cong 1 + \frac{1}{2} \{A_r [\cos(t^* - x^*) + x^* \sin(t^* - x^*)]\}^2 \end{aligned}$$

which simplifies the algebra considerably

$$u^* = x^* - s^* \cong \frac{-A_r^2}{2} \int_0^{x^*} [\cos(t^* - \xi) + \xi \sin(t^* - \xi)]^2 d\xi$$

We integrate, and expand the terms to separate time and space variables to obtain the longitudinal deflection

$$u^* \cong \frac{-A_r^2}{2} \left\{ \begin{array}{l} \frac{1}{6}x^{*3} + \frac{1}{4}x^* + \frac{1}{2}x^{*2} \cos x^* \sin x^* + \frac{1}{2}x^* \sin^2 x^* - \frac{1}{4} \cos x^* \sin x^* \\ + \cos^2(t^*) \left\{ -x^{*2} \cos x^* \sin x^* + x^* \cos^2 x^* - \frac{1}{2}x^* + \frac{1}{2} \cos x^* \sin x^* \right\} \\ + \cos(t^*) \sin(t^*) \left\{ x^{*2} \cos^2 x^* + x^* \cos x^* \sin x^* - \frac{1}{2}x^{*2} + \frac{1}{2} \sin^2 x^* \right\} \end{array} \right\}$$

### 5.2.3 Motion-induced Tension

The acceleration vector of a point on the flag is

$$\vec{a} = \frac{\omega^2}{\kappa} \left[ \frac{d^2 u^*}{dt^{*2}} \vec{i} + \frac{d^2 w^*}{dt^{*2}} \vec{k} \right]$$

Inserting the values from our mode-shape specification

$$\frac{d^2 w^*}{dt^{*2}} = -A_r \{ \cos t^* \{ x^* \cos x^* \} + \sin t^* \{ x^* \sin x^* \} \}$$

The direction cosines for the local direction of the flag are

$$\begin{aligned} \vec{ds} &= \frac{(dx) \vec{i} + (dw) \vec{k}}{\sqrt{(dx)^2 + (dw)^2}} \cong (1) \vec{i} + \left( \frac{dw}{dx} \right) \vec{k}, \text{ if } (dw/dx)^2 \ll 1 \\ &\cong (1) \vec{i} + A_r \left\{ \begin{array}{l} \cos t^* \{ \cos x^* - x^* \sin x^* \} \\ + \sin t^* \{ \sin x^* + x^* \cos x^* \} \end{array} \right\} \vec{k} \end{aligned}$$

The component of the acceleration of the mass-per-unit-area in the local plane of the flag is balanced by the change in tension

$$\begin{aligned} \frac{dT}{dx} &\cong \frac{dT}{ds} = m_{flag} \vec{ds} \cdot \vec{a} \\ &\cong -A_r^2 m_{flag} \frac{\omega^2}{\kappa} \left\{ \begin{array}{l} \left\{ \frac{1}{2}x^* + \frac{1}{2} \cos x^* \sin x^* \right\} \\ + \cos^2 t^* \left\{ -\cos x^* \sin x^* \right\} \\ + \cos t^* \sin t^* \left\{ -\sin^2 x^* \right\} \end{array} \right\} \end{aligned}$$

which we can integrate to obtain tension.

### 5.2.4 Cumulative motion-induced tension

The tension-per-unit width is

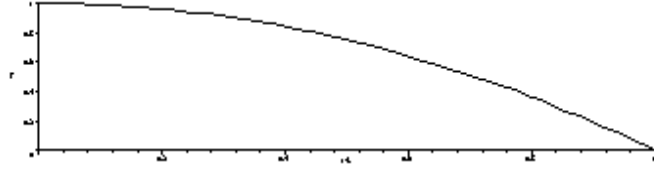
$$\begin{aligned} T &\cong -A_r^2 m_{flag} \frac{\omega^2}{\kappa} \cdot \frac{1}{\kappa} \int_{L^*}^{x^*} \left( \frac{1}{2} \cos(t^* - \xi) \sin(t^* - \xi) + \frac{1}{2} \xi - \frac{1}{2} \cos t^* \sin t^* \right) d\xi \\ &\cong A_r^2 m_{flag} \frac{\omega^2}{\kappa^2} \left\{ \begin{array}{l} \frac{1}{4} L^{*2} - \frac{1}{4} x^{*2} \\ + \cos 2t^* \left\{ \left( \frac{1}{8} \cos 2L^* - \frac{1}{8} \cos 2x^* \right) \right\} \\ + \sin 2t^* \left\{ \left( \frac{1}{8} \sin 2L^* - \frac{1}{8} \sin 2x^* \right) - \left( \frac{1}{4} L^* - \frac{1}{4} x^* \right) \right\} \end{array} \right\} \end{aligned}$$

with a *maximum value* at the leading edge ( $x = 0$ )

$$T_{\max} \cong A_r^2 m_{flag} \frac{\omega^2}{\kappa^2} \left\{ \frac{1}{4} L^{*2} + \frac{1}{8} \sqrt{(2 - 2 \cos 2L - 4L \sin 2L + 4L^2)} \cos(2t^* - \phi) \right\}$$

The distribution of the *time-averaged* tension is

$$[T]_{\text{avg}} \cong A_r^2 m_{flag} \frac{\omega^2}{\kappa^2} \left\{ \frac{1}{4} L^{*2} - \frac{1}{4} x^{*2} \right\}$$



a more nearly uniform, less “peaked” distribution than friction drag, with the **time-average maximum** value at the flagpole of

$$[T_{\max}]_{\text{avg}} \cong A_r^2 m_{flag} \frac{\omega^2}{\kappa^2} \left\{ \frac{1}{4} L^{*2} \right\}$$

The amplitude of the *fluctuations* in tension at the flagpole is

$$[T_{\max}]_{\text{AC}} \cong A_r^2 m_{flag} \frac{\omega^2}{\kappa^2} \left\{ \frac{1}{8} \sqrt{(2 - 2 \cos 2L^* - 4L^* \sin 2L^* + 4L^{*2})} \cos(2t^* - \phi) \right\}$$

We can determine bounds and conclude that the amplitude of the fluctuations is guaranteed to be less than the average (no possibility of “negative tension”) if

$$L > \frac{\lambda}{4}.$$

This condition is met by typical flags, which are several wave-lengths long. When the flag is many wave-lengths long, then  $L^* \gg 1$ , and the fluctuations approach  $1/L^*$  of the average value.

### 5.2.5 Comparison with D. Thoma

Thoma<sup>9</sup> treated a perfectly flexible inextensible rope of uniform mass-per-unit-length  $m_{flag}$ , fastened at  $x = 0$  and free at  $x = L$ , and acted on by arbitrary normal forces. For the average tension at the attachment point, he obtained

$$[T_{(0)}]_{\text{avg}} = \frac{1}{2} m_{flag} [V_{tip}^2]_{\text{avg}}$$

<sup>9</sup>D. Thoma (1939), "Das schlenkernde Seil" (The oscillating rope), *Z. Angew. Math. Mech.* (*ZAMM*) Vol. 19, Nr. 5 (Oktober 1939), pages 320–321.

This result did not require the simplifications obtained in our series expansion by assuming  $|dw/dx| \ll 1$ , but is applicable to large deflections and slopes. The algebraic difficulties are now shifted to obtaining the magnitude of the tip velocity. For our traveling and monotonically growing wave, we can simplify and *estimate* the value of the tip velocity from

$$V_{tip}^2 = \dot{w}_{tip}^2 + \dot{u}_{tip}^2 \cong \dot{w}_{tip}^2$$

and obtain the same result for the time-averaged maximum (*i.e.*, at  $x = 0$ ) value as before.

### 5.3 Experimental Data

Although experimental data were obtained by Taneda<sup>10</sup> and others, the reported results are not sufficiently detailed to test this result; we are planning wind-tunnel tests at Oklahoma State University to fill-in the gaps in the data.

Getting away from the hydrodynamically induced mass (which is not exact near the leading and trailing edges), the complete governing equation for the flag is

$$m_{flag} \frac{\partial^2 w}{\partial t^2} - T \frac{\partial^2 w}{\partial x^2} - \frac{\partial T}{\partial x} \frac{\partial w}{\partial x} = p_a(x, t) - p_b(x, t)$$

where  $p$  is the pressure difference across the flag. Having assumed the motion  $w$ , we can obtain this pressure difference and compare it with the pressures obtained from the unsteady ideal flow around the flag for the same boundary location  $w$ .

### 5.4 Numerical Computations

Translated into a non-linear governing equation, and using the curvilinear coordinate  $s$  along the path of the inextensible flag, the PDE to be programmed into the structural numerical simulation becomes<sup>11</sup>

$$\begin{aligned} & m_{flag} \frac{\partial^2 w}{\partial t^2} \\ & - T_{long} \frac{\partial^2 w}{\partial s^2} \left[ 1 + \frac{3}{2} \left( \frac{\partial w}{\partial s} \right)^2 \right] - m_{flag} \frac{\partial^2 w}{\partial s^2} \int_s^L \int_0^s \left( \left( \frac{\partial^2 w}{\partial t \partial s} \right)^2 + \frac{\partial w}{\partial s} \frac{\partial^3 w}{\partial t^2 \partial s} \right) ds ds \\ & - \frac{\partial T_{long}}{\partial s} \frac{\partial w}{\partial s} \left[ 1 + \frac{1}{2} \left( \frac{\partial w}{\partial s} \right)^2 \right] \mp m_{flag} \frac{\partial w}{\partial s} \int_0^s \left( \left( \frac{\partial^2 w}{\partial t \partial s} \right)^2 + \frac{\partial w}{\partial s} \frac{\partial^3 w}{\partial t^2 \partial s} \right) ds \\ & + EI \left\{ \frac{\partial^4 w}{\partial s^4} \left[ 1 + \left( \frac{\partial w}{\partial s} \right)^2 \right] + 4 \frac{\partial w}{\partial s} \frac{\partial^2 w}{\partial s^2} \frac{\partial^3 w}{\partial s^3} + \left( \frac{\partial^2 w}{\partial s^2} \right)^3 \right\} \\ & = \Delta p \end{aligned}$$

<sup>10</sup>S. Taneda, "Waving Motion of Flags," *Journal of the Physical Society of Japan*, Vol. 24 (1968), No. 2, pp. 392-401.

<sup>11</sup>see Michael P. Paidoussis, *Fluid-Structure Interactions: Slender Structures and Axial Flow Volume 1*, Academic Press, San Diego, California, 1998, ISBN 0-12-544360-9.

and a complementary Computational Fluid Dynamics program must be implemented for evaluating  $\Delta p$ .

## 6 Suggested Reading

1. R. Skutch, "Über die Bewegung eines gespannten Fadens, welches gezwungen ist, durch zwei feste Punkte, mit einer constanten Geschwindigkeit zu gehen, und zwischend denselben in Transversal-Schwingungen von geringer Amplitude versetzt wird," *Annalen der Physik und Chemie*, Vol. 61 (1897), pp. 190–197 (in the Hessische Landes- und Hochschulbibliothek **LHB**, Schloss: Zs 3201).
2. G.F. Carrier, "The Spaghetti Problem," *Amer. Math. Monthly*, Vol. 56 (1949), pp. 669–672 (in **Mathe**, Schlossgartenstr. 7, S2/15 Room 240: Regal 10).
3. R. Barakat, "Transverse Vibrations of a Moving Thin Rod," *Journal of the Acoustical Society of America*, Vol. 43 (1968), No. 3, pp. 533–539 (in **Mechanik**, Hochschulstr. 1, S1/03 Room 362: Z 14).
4. A. Simpson, "Transverse Modes and Frequencies of Beams Translating Between Fixed End Supports," *Journal of Mechanical Engineering Science*, Vol 15 (1973), No. 3, pp. 159–164 (**LHB**, Schloss: Zl 4489).
5. H.M. Nelson, "Transverse Vibrations of a Moving Strip," *Journal of Sound and Vibration*, Vol. 65 (1979), No. 3, pp. 381–389 (**Mechanik**: Z 226).
6. M.S. Triantafyllou, "Linear Dynamics of Cables and Chains," *Shock. Vib. Dig.*, Vol 16 (1984), pp. 9–14 (Maschinendynamik **MADY**, Lichtwiese, Petersenstr. 30, L1/01 Room 549: 17/113).
7. M.S. Triantafyllou, "The Dynamics of Translating Cables," *Journal of Sound and Vibration*, Vol 103 (1985), No. 2, pp. 171–182 (**Mechanik**: Z 226).
8. A. Pramila, "Sheet Flutter and the Interaction between Sheet and Air," *TAPPI Journal*, Vol. 69 (1986), No. 7, pp. 70–74 (**LHB**, Schloss: Zs 8562).
9. J.G. Simmonds & L. Mansfield, "The Reverse Spaghetti Problem: Drooping Motion of an Elastica Issuing from a Horizontal Guide," *Trans. ASME, Journal of Applied Mechanics*, Vol. 54, No. 1.(March 1987), pp. 147–150 (**Mechanik**).
10. J. Niemi & A. Pramila, "FEM-Analysis of Transverse Vibrations of an Axially Moving Membrane Immersed in Ideal Fluid," *Intl. J. Numer. Methods Engrg.*, Vol. 24 (1987), No. 12, pp. 2301–2313 (**MADY**: 17/83).